

Filtered Talbot lens: Producing $\lambda/2n$ -periodic atomic patterns with standing wave fields having period λ

J. L. Cohen, B. Dubetsky, and P. R. Berman

Physics Department, University of Michigan, Ann Arbor, MI 48109-1120

J. Schmiedmayer

*Institut für Experimentalphysik, Universität-Innsbruck,
Technikerstrasse 25, A-6020 Innsbruck, Austria*

(September 4, 2021)

We propose a scheme to create high-contrast, periodic atom density distributions having period $\lambda/2n$ using the Talbot effect, where λ is the wave length of the optical fields that scatter the atoms and n is a positive integer. This *filtered Talbot lens* is comprised of two standing-wave optical fields. An atomic beam propagates perpendicular to the fields. The first field, which is far-detuned from the atomic transition frequency, acts as an array of lenses that focuses the atoms. The second field, positioned at the atom optical focus of the first, is resonant with the atomic transition frequency and acts as an amplitude mask, leaving unperturbed only those atoms that pass through its nodes. At distances following the interaction with the second field that are equal to an integral fraction of the Talbot length, atomic density gratings having period $\lambda/2n$ are formed.

03.75.Be, 32.80.Lg, 39.20.+q

I. INTRODUCTION

Over the past several years, considerable progress has been made in the manipulation of atoms by optical fields. One important application of this new technology is the focusing and deposition of atoms on substrates [1,2]. Using standing wave optical fields having wavelength λ , one has been able to write a periodic array of lines or dots having period $\lambda/2$. The atomic "lines" or "dots" themselves have widths w that are very small compared with $\lambda/2$; widths (half width at half maximum) as small as 6.5 nm have been achieved [3]. With such a resolution, one can envision writing structures having periods as small as $\lambda/2n$, where n , the atomic grating order, can be as large as

$$n_{\max} \sim \lambda/4w \sim 25. \quad (1)$$

Although periods as small as $\lambda/2n_{\max}$ are consistent with the resolution achieved to date, it is not obvious how one can use optical fields having wavelength λ to produce such periodic structures. For example, focusing by standing wave fields results in periods equal to $\lambda/2$, or possibly $\lambda/4$ if cross-polarized counterpropagating waves are used [4]. A similar periodicity can be expected using optical masks [5], in which only those atoms passing through the nodes of a standing wave field are registered on a substrate.

There have been a number of proposals for producing *sub- λ* or *higher-order* atomic density gratings, which necessarily involve nonlinear interactions of the atoms with the fields. Atom interference [6] allows one to exploit photon echo techniques to isolate higher order gratings at specific focal planes following the interaction of an atomic beam with two or more standing wave fields [7,8].

High-order Bragg scattering of an atomic beam by standing wave fields has produced structures with periods as small as $\lambda/6$ [9]. Counterpropagating waves, detuned from one another by an appropriate ratio, can be used to create arbitrarily high order gratings with good contrast [10]. It is even possible to achieve higher order gratings using the standard focusing or optical mask geometries, if one is able to exploit the Talbot or self-imaging effect [11]

In atom optics the Talbot effect was observed using microfabricated structures to scatter atoms [12]. When atoms propagating along the z axis pass through a microfabricated structure having period $\lambda/2$ in the x -direction, the atomic spatial distribution becomes a periodic function of z having period equal to the Talbot length $L_T = \lambda^2/2\lambda_{dB}$, where $\lambda_{dB} = h/Mu$ is the atomic de Broglie wavelength, and M and u are atomic mass and speed, respectively. In other words, self images of the microfabricated grating are produced at integral multiples of the Talbot length. Moreover, for a microfabricated structure with duty cycle f (ratio of opening to period), periodic structures having order as high as $\lambda/2f$ can be produced at integral fractions of the Talbot length [13]. Using this technique, 7th order gratings have been observed [14] using a metastable He beam passing through a microfabricated structure having period $\lambda/2 = 6.55 \mu$ and duty cycle $f = 0.1$.

Instead of microfabricated structures, one can use an optical mask to act as an amplitude grating for a beam of metastable atoms. In a typical experiment [5], a metastable atomic beam is sent through a standing wave field that is resonant with a transition originating on the metastable level (see Fig. 1). If the upper level is excited by the field, it decays to the ground state. By using a

substrate that is sensitive only to metastable atoms, one exposes the substrate only to those atoms which pass through the nodes of the field. Thus, for metastable atoms the strong standing wave field acts as a microfabricated structure with a small duty cycle. Experimentally, an atomic grating having period of order 200 nm ($\lambda/4$) was created using this effect when a metastable Ar beam was passed through an optical mask [15]. An alternative, non-lithographic detection scheme that probes the lower level population may also be possible [16].

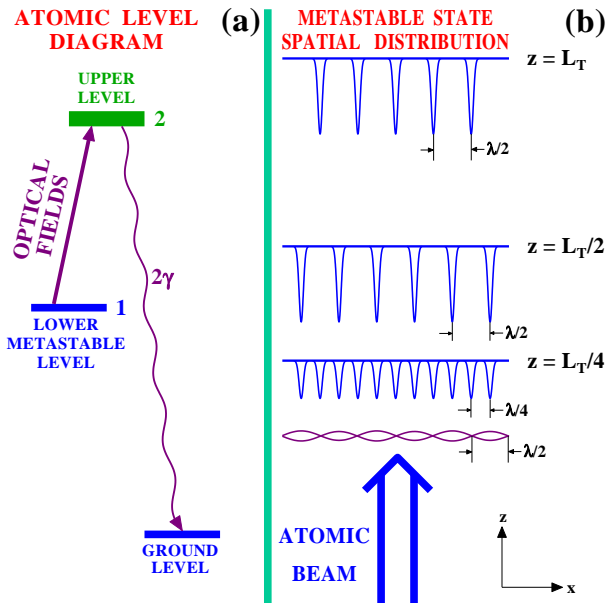


FIG. 1. Talbot effect and fractional self-images using an optical mask. When a beam of metastable atoms having the level scheme shown in (a) passes through the resonant standing wave field shown in (b), only atoms moving within the narrow vicinity of the field nodes remain in level 1, producing a metastable atomic density grating (not shown in the figure) having period $\lambda/2$ immediately following the interaction. Further free evolution of the atomic wave function results in a first-order self-image at the Talbot distance $z = L_T$, a $\lambda/4$ spatial shift of this density at the distance $z = L_T/2$, a second-order self-image at the distance $z = L_T/4$, and higher-order images at the fractional Talbot distances $z = L_T/m$, for integer m .

Optical masks give a high fringe contrast, but low deposition rate, since most of the atoms pass through high field regions and are not recorded on the substrate. To overcome this problem without an optical mask, one might try to combine the Talbot effect with the focusing of atoms by a far-detuned standing wave field. The field, which is also aligned along the x axis, acts as a series of lenses. The centers of the lenses are located at the minima of the optical potential produced by the field, and the focal length of each lens is denoted by z_f . If these focused atoms were equivalent to atoms passing through an *amplitude transmission grating at the focal plane*, one would expect that, as a result of the Talbot effect, high-

contrast, high-order images of the periodic focal pattern would be formed at distances

$$z_m = z_f + L_T/m. \quad (2)$$

from the field. Janicke and Wilkens [17] carried out numerical calculations to obtain some evidence for this effect. A more detailed analysis [18], however, reveals that *the background density between the focused atoms seriously degrades the fractional Talbot effect*.

It might seem strange that the relatively small background density between the focal spots can lead to a serious degradation of the fractional Talbot signal. To understand the origin of this effect, it is helpful to return to the theory of the fractional Talbot effect [13]. If a wave function $\psi(x, z_f)$ is prepared at $z = z_f$ having period d , then at a fractional Talbot distance L_T/m from this plane, this wave function is mapped into a set of n copies shifted from one another along x by a distance d/n (with $n = m$ or $m/2$). The total wave function is a linear superposition of these copies with coefficients having the same absolute value *but different phases*. After squaring the wave function to obtain the atomic density, one finds that the different phases are responsible for the degradation of the fractional Talbot images. In the case of focusing by an off-resonance field, one finds that the tail of the wave function of one of the copies interferes with the peak of the wave function of another copy. This is a strong effect. A tail to peak ratio of 0.1 in the wave function at $z = z_f$ implies a ratio of background to peak density of 0.01 at $z = z_f$. However, at a fractional Talbot distance from $z = z_f$, interference between the tail and peak of the wave function can result in changes to the atomic density that can deviate by as much as 20% from the density that would have been produced in the absence of any background density.

One way to avoid such interference effects is to minimize or eliminate the background density. If a plane matter wave is incident on a microfabricated grating or periodic amplitude mask having duty cycle f , one period of the wave function immediately following the mask consists of a peak having width df and a vanishing background density having width $(1-f)d$. At a fractional Talbot distance L_T/m from this plane, there will be no spatial overlap (and no interference) of the n copies ($n = m$ or $m/2$) of the wave function, provided that $n < 1/f$. If this condition is satisfied, a "perfect" fractional Talbot effect is produced.

To improve the quality of the fractional Talbot images, one can place a mask in the path of the atoms just before they interact with the focusing field. The mask reduces the aperture of each "lens" in the standing wave focusing field, resulting in reduced spherical aberration and a reduction in background density [19]; however, just as in the case of optical masks, a significant decrease in beam flux results. In this paper, we combine off-resonant focusing with an optical mask placed at the focal plane of the off-resonant field. The mask acts as a spatial filter for the focused atoms that removes most of the background

atoms between the focal spots. Thus, the atomic beam flux is maintained while the degradation of the fractional Talbot effect is avoided. As such, one can expect this *filtered Talbot lens* (FTL) to produce high density images of reduced periodicity at integral fractions of the Talbot distance from the focal plane. It is important to note that the wave fronts need not be planar at the mask openings. As long as the waves incident on the *focusing* field are nearly planar, the matter waves converging at the focal plane are coherent. This coherent matter wave impinging on the mask produces a very different diffraction pattern than that of an *incoherent* superposition of plane waves incident from different directions. An incoherent superposition of waves would not produce a fractional Talbot image on averaging over all directions of the incident wave, whereas a coherent incident beam can produce a "perfect" fractional Talbot effect if the duty cycle of the mask is sufficiently small.

We proceed below to examine this possibility in more detail.

II. FILTERED TALBOT LENS

A beam of atoms having the level structure shown in Fig. 1 interacts with two standing wave optical fields that drive the 1 – 2 transition. The first field, located at $z = 0$, is far-detuned from the atomic resonance and focuses the atoms at the plane $z = z_f$. The second field, shown in Fig. 1 and located at $z = z_f$, is resonant or nearly resonant with the atoms. The atoms move with velocity $\mathbf{u} = u\hat{\mathbf{z}}$, and the 1 – 2 transition frequency is denoted by ω . In the atomic rest-frame ($z = ut$), the fields appear as two pulses with electric field vectors given by

$$\mathbf{E}(x, t) = \hat{\mathbf{y}} \frac{1}{2} \sum_{j=1,2} E_j e^{-i\Omega_j t} g_j(t - t_j) \times \cos[kx + (1 - j)\pi/2] + c.c., \quad (3)$$

where $k = q/2$ is a propagation constant, $t_1 = 0$, $t_2 = t_f = z_f/u$, and E_j and Ω_j are the amplitude and frequency, respectively, of the j th pulse. We assume that the pulse envelopes $g_j(t)$ are smooth functions of t centered at $t = 0$, that both pulses have the same duration τ , and that $\tau \ll t_f$. *During* the interaction with the j th pulse, the atomic state vector in the interaction representation

$$\psi(x, t) = \begin{pmatrix} \psi_2(x, t) \\ \psi_1(x, t) \end{pmatrix}$$

evolves as

$$i\partial\psi(x, t)/\partial t = (\mathbf{V}_j - i\gamma)\psi(x, t), \quad (4)$$

and *between or after* the pulses the state vector evolves as

$$i\partial\psi(x, t)/\partial t = -\frac{\hbar}{2M} \frac{\partial^2\psi(x, t)}{\partial x^2} - i\gamma\psi(x, t), \quad (5)$$

where $\hbar\mathbf{V}_j$ is the interaction Hamiltonian,

$$\mathbf{V}_j = \begin{pmatrix} 0 & \chi_j g_j(t - t_j) e^{-i\Delta_j t} \\ \chi_j^* g_j^*(t - t_j) e^{i\Delta_j t} & 0 \end{pmatrix} \cos(kx), \quad (6)$$

$\chi_j = -\mu E_j/2\hbar$ is a Rabi frequency, $\Delta_j = \Omega_j - \omega$ is an atom-field detuning, and μ is a dipole moment matrix element. The relaxation matrix

$$\gamma = \begin{pmatrix} \gamma & 0 \\ 0 & 0 \end{pmatrix} \quad (7)$$

corresponds to a case for which the lower state is metastable and the upper state population decays with rate 2γ to level 0 *outside* of the 1 – 2, two-level subspace. The decay rate of state |1> has been set equal to zero under the assumption that its lifetime is much greater than the Talbot time,

$$T = L_T/u = \lambda^2/(2u\lambda_{dB}) = 2\pi/(\hbar q^2/2M), \quad (8)$$

which is the relevant time scale in these focusing experiments. In Eq. (4) we have invoked the Raman-Nath approximation and neglected terms associated with the kinetic energy of the atoms *during* the atom-field interaction.

Before interacting with the first field, it is assumed that the collimated beam can be approximated by a plane wave state in the x direction having x -component of momentum $p = 0$. If the atoms enter the first field zone in state |1>, then the net effect of the far-detuned first pulse [$|\Delta_1| \gg \max(|\chi_1|, \gamma)$] is to produce a phase modulation of the atomic lower state wave function,

$$\psi_1(x, t = 0^+) = \exp[i(\theta/2) \cos(qx)], \quad (9)$$

where

$$\theta = -\frac{|\chi_1|^2}{\Delta_1} \int_{-\infty}^{\infty} dt_1 |g_1(t_1)|^2 \quad (10)$$

is a pulse area. We assume that $\Delta_1 < 0$, resulting in $\theta > 0$.

Following the action of the first pulse, the lower state wave function evolves freely so that just before the second pulse acts, one has [18]

$$\psi_1(x, t = t_f^-) = \sum_{s=-\infty}^{\infty} i^s J_s(\theta/2) \exp(-is^2\omega_q t_f + isqx), \quad (11)$$

where $J_s(x)$ is a Bessel function of order s and

$$\omega_q = \hbar q^2/2M = 2\pi/T \quad (12)$$

is a two-photon recoil frequency. When $\gamma t_f \gg 1$, one can neglect the small upper state amplitude at $t = t_f$. The atoms are assumed to be focused at the time t_f (distance $z_f = ut_f$) to lines centered at $x = 2\pi s/q$ for integer s .

To determine the effect of pulse 2, one must solve Eq. (4) with $j = 2$, subject to the initial condition

$$\psi_- = \begin{pmatrix} 0 \\ \psi_1(x, t = t_f^-) \end{pmatrix}. \quad (13)$$

An analytic solution can be obtained if we assume that $|\dot{g}_2(t)/g_2(t)| \ll \gamma$ or

$$\tau \gg \gamma^{-1}. \quad (14)$$

Condition (14) is desirable as it guarantees that atoms will have time to decay out of the two-state subspace during the interaction with the second field pulse. Moreover, it is sufficient to satisfy the adiabatic condition

$$\tau \gg \min(\gamma^{-1}, |2\chi_2|^{-1}, |\Delta_2|^{-1}). \quad (15)$$

As a result, the pulse turns on sufficiently slowly to ensure that instantaneous eigenstates of the complex "Hamiltonian", $\hbar(\mathbf{V}_2 - i\gamma)$ are approximate eigenstates of the system. In this manner the lower state wave function following the second pulse's action is given by

$$\psi_1(x, t = t_f^+) \approx \eta(x)\psi_1(x, t = t_f^-), \quad (16)$$

where

$$\eta(x) = \exp \frac{i}{2} \int_{-\infty}^{\infty} dt_1 [\Delta_2 + i\gamma - ((\Delta_2 + i\gamma)^2 + 4|\chi_2 g_2(t_1)|^2 \sin^2(kx))^{1/2}] \quad (17)$$

is the transmission function associated with the optical mask.

Following the second pulse, the lower state again evolves freely. When the masking field is on exact resonance ($\Delta_2 = 0$) and weak ($|\chi_2|/\gamma \ll 1$), one finds

$$\eta(x) = \exp[-\beta \sin^2(kx)], \quad (18)$$

where

$$\beta = \frac{|\chi_2|^2}{\gamma} \int_{-\infty}^{\infty} dt_1 |g_2(t_1)|^2 \quad (19)$$

is the area associated with pulse 2. Expanding expression (18) in plane waves and keeping in mind that each plane wave e^{isqx} acquires the time-dependent phase factor $e^{-is^2\omega_q(t-t_f)}$ for $t > t_f$, one obtains

$$\psi_1(x, t) = e^{-\beta/2} \sum_{s_1, s_2} i^{s_1} J_{s_1}(\theta/2) I_{s_2}(\beta/2) \exp \left\{ -i\omega_q \left[s_1^2 t_f + (s_1 + s_2)^2 (t - t_f) \right] + i(s_1 + s_2)qx \right\}, \quad (20)$$

where $I_s(x)$ is a modified Bessel function of order s . From this expression, using an addition theorem for Bessel functions, one finds that the atom density, $\rho(x, t) = |\psi(x, t)|^2$, is given by

$$\rho(x, t) = e^{-\beta} \sum_{s_1, s_2} J_{s_1} \{ \theta \sin[\omega_q(s_1 t + s_2(t - t_f))] \} \times I_{s_2} \{ \beta \cos[\omega_q(s_1 + s_2)(t - t_f)] \} e^{i(s_1 + s_2)qx}. \quad (21)$$

Expressions (11), (20), and (21) are convenient for numerical evaluation of the atomic wave function and density. On the other hand, they do not reveal in any transparent fashion the density peaks at the focal plane $t = t_f$ and the high-order harmonic density patterns at the fractional Talbot times

$$t_m = t_f + T/m. \quad (22)$$

Both of these features are more readily apparent if we follow alternative approaches. First, instead of Eq. (11), one can use approximate expressions for the focal plane position and atom density profile in the asymptotic limit of $\sqrt{\theta} \gg 1$ [18],

$$t_f \sim \omega_q^{-1} \theta^{-1} \left(1 + 1.27\theta^{-1/2} \right), \quad (23a)$$

$$\rho(x, t_f) \sim \sum_{s=-\infty}^{\infty} \frac{\sqrt{3\theta}}{\pi} \times \left| f \left(3^{1/4} \theta^{3/4} (qx - 2\pi s), -2.20 \right) \right|^2, \quad (23b)$$

$$f(\tilde{x}, \tilde{\omega}) = \int_{-\infty}^{\infty} d\xi \exp(-i\tilde{x}\xi + i\tilde{\omega}\xi^2 + i\xi^4). \quad (23c)$$

Equation (23b) is valid within the small regions near the standing wave nodes, $|x - s\lambda/2| \lesssim \lambda\theta^{-3/4}$.

Second, one can also obtain alternative expressions for the atomic density at the fractional Talbot times. Equation (21) is valid for arbitrary $t > t_f$. However, if the time is restricted to be a rational fraction of the Talbot time after the focus [20],

$$t = t_f + (\ell/m)T, \quad (24)$$

for integer ℓ and m , a derivation, similar to the one given in Ref. [13], leads to

$$\psi_1(x, t) = \sum_{s=0}^{m-1} a_s \psi_1(x - s\lambda/2m, t = t_f^+), \quad (25a)$$

$$a_s = (2im)^{-1} \sum_{s'=0}^{\ell} \exp \left[i\pi (s + ms')^2 / 2m \right], \quad (25b)$$

valid in the interval $0 \leq x < \lambda/2$. The wave function at these times (24) appears as a superposition of m scaled

images of the filtered wave function at the focal time. In forming the atomic density,

$$\rho(x, t) = |\psi_1(x, t)|^2, \quad (26)$$

it is possible for different terms in the sum over s to interfere. (In the absence of the optical mask ($\beta = 0$), these interference terms cause significant density oscillations that ruin the fractional self-image of the atoms focused by the far-detuned field.) However, if the optical mask at t_f produces very narrow structures with an effective duty cycle much less than unity, then the interference terms are unimportant and the density reduces to

$$\rho(x, t) = \sum_{s=0}^{m-1} |a_s|^2 \left| \psi_1(x - s\lambda/2m, t = t_f^+) \right|^2. \quad (27)$$

When valid, the spatial distribution (27) becomes an exact n th-order image of the density at t_f when all non-zero coefficients (25b) have the same absolute value. This can occur at the fractional Talbot times

$$t_m = t_f + (T/m), \quad (28)$$

with $\ell = 1$ in Eq. (24). At these times, the coefficients become

$$|a_s| = (2/m)^{1/2} \begin{cases} |\cos(m\pi/4)|, & \text{for even } s \\ |\sin(m\pi/4)|, & \text{for odd } s \end{cases} \quad (29)$$

Three cases can be distinguished [13]:

$$(a) \quad m = 2n' + 1, \quad (30a)$$

$$(b) \quad m = 2(2n' + 1), \quad (30b)$$

$$(c) \quad m = 4n', \quad (30c)$$

where n' is a positive integer. In case (a), $|a_s|^2 = 1/m$ for all s , leading to atomic densities having period $\lambda/[2(2n' + 1)]$. In case (b), $|a_s|^2 = 2/m$ for odd s and $|a_s|^2 = 0$ for even s , leading to atomic densities having period $\lambda/[2(2n' + 1)]$ but that are shifted by half a period from those of case (a). In case (c), $|a_s|^2 = 2/m$ for even s and $|a_s|^2 = 0$ for odd s , leading to densities having period $\lambda/4n'$.

For the FTL scheme to produce high-quality, high-contrast fractional self-images, it is sufficient that three conditions are met. First, the focused atoms at t_f must have a large density ($\rho(x, t_f) \gg 1$) at the positions $x = 2\pi s/q$. For $\theta \gg 1$, the peak density can be estimated to grow as $3.83\theta^{1/2}$ according to an analysis of Eq. (23b) [18]. Second, the focal spot size $2w \approx 0.118\lambda\theta^{-3/4}$ [18] should be less than $\lambda/2m$ for case (a) and less than λ/m for cases (b) and (c). Thus, the effective duty cycle of the focused atom density over the $\lambda/2$ period is

$$f \simeq 4w/\lambda \approx 0.237\theta^{-3/4}, \quad (31)$$

giving a maximum possible grating order on its own of

$$n_{\max} \simeq f^{-1} \approx 4.22\theta^{3/4}. \quad (32)$$

Third, for Eq. (27) to be valid so that interference terms in the focused atom wave function do not degrade the fractional images at later times, the optical mask should only pick out the density peaks and clip the tails of the unavoidable background wave function between the peaks. If we wish to use most of the focused atoms, the optical mask slit width or opening size δx should not be smaller than the focused atom spot size $2w$. From Eq. (18), it follows that the transmission function near the nodes for $|\chi_2|/\gamma \ll 1$ and $\Delta_2 = 0$ is $\eta(x) \simeq \exp[-\beta(kx)^2]$, from which we can estimate that the effective opening size δx is

$$\delta x \simeq \left(\frac{\ln 2}{\beta} \right)^{1/2} \frac{\lambda}{\pi} \approx 0.265 \frac{\lambda}{\beta^{1/2}}.$$

Setting $\delta x \gtrsim 2w$, one finds the upper limit for β

$$\beta < 5.04\theta^{3/2}. \quad (33)$$

To establish a lower limit for β , one must examine Eqs. (11, 18, 25, 27) numerically for given values of θ and m . We have found that a value of β an order of magnitude smaller than the upper limit given by Eq. (33) can still give rise to high contrast gratings.

III. DISCUSSION

In Fig. 2 we compare the atomic spatial distributions at the fractional Talbot lengths when the focusing and masking fields each act alone and when they are combined as detailed above. This plot was obtained numerically using Eqs. (11) and (25) in (26) for $\theta = 10$ and $\beta = 40$. [Alternatively, one can evaluate the density using Eq. (21). This equation must be used for distances following the focal plane that are not a rational fraction of the Talbot time.] The effective opening size of the optical mask (pulse 2) is larger than the spot size of the focused atomic beam but still sufficiently narrow to filter out the majority of background atoms in the tail of the wave function. From Eq. (23a) one finds $t_f \approx 0.140\omega_q^{-1}$, but we use the more precise value $t_f \approx 0.146\omega_q^{-1}$, obtained numerically in Ref. [18]. The FTL produces high-contrast, higher order atomic gratings at the fractional Talbot times. The mask alone also produces such periodic structures but with severely reduced contrasts and larger spot sizes. The focusing field acting alone produces narrow structures at the fractional Talbot distances, but the density's overall periodicity remains equal to $\lambda/2$ as opposed to forming a self-image of reduced periodicity.

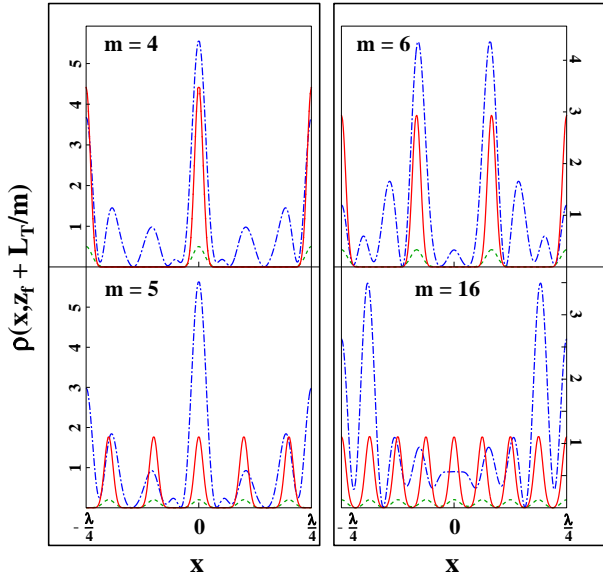


FIG. 2. Filtered Talbot lens production of high-order atomic density patterns (solid lines) at distances $z_f + L_T/m$ for a mask parameter $\beta = 40$ in the weak field regime $|\chi_2|/\gamma \ll 1 \ll \gamma\tau$. For comparison, we show the spatial distributions of the metastable atomic density produced by the optical mask alone at the fractional Talbot distances (dashed lines) and by the focusing field alone at the fractional Talbot distances from the focal plane (dot-dashed lines). For all plots, the focusing field area θ is equal to 10.

Within the confines of the Raman-Nath approximation, it might be difficult to achieve a value $\beta = 40$ if $|\chi_2| \ll \gamma$. For example, when $|\chi_2|/\gamma \sim 0.1$, one needs $\gamma\tau$ to be as large as 4×10^3 . For $\gamma/\omega_q \sim 10^3$ this implies values of $\omega_q\tau > 1$, which are inconsistent with the Raman-Nath approximation. To avoid this difficulty, smaller values of $\gamma\tau$ can be used with larger Rabi frequencies. Let us assume that field 2, the standing wave mask, is a resonant, rectangular pulse with $|\chi_2|/\gamma \gg 1$ and that the adiabatic condition (15) is satisfied [21]. Then, except in the vicinity of the nodes, the transmission function (17) is

$$\eta(x) = \exp(i|\chi_2\tau \sin(kx)| - \gamma\tau/2). \quad (34)$$

From this expression, a value of $\gamma\tau \sim 3 - 4$ is enough to attenuate the tails of the focused atoms with an accuracy of several percent. Near the nodes, $|\chi_2 \sin(kx)| \ll \gamma$, and Eq. (19) is still valid. As a result, large values of an effective β are possible for $|\chi_2|/\gamma \gg 1$ even if $\gamma\tau$ is on the order of unity.

In Fig. 3 we plot the atom density profiles at fractional Talbot distances with $\gamma\tau = 4$ and $\theta = 10$. The plot has been obtained by combining Eqs. (11), (16), (17), and (25) [22]. We have found that the amplitudes of the different peaks between $x = 0$ and $x = \lambda/2$ in the fractional Talbot effect oscillate slightly as a function of $|\chi_2|$. The origin of these Rabi-like oscillations is an interference of the m terms in Eq. (25a), each of which has a different phase that depends on the Rabi frequency χ_2 . For each m

we have chosen a value of the parameter $|\chi_2|\tau$ that minimizes these oscillations to provide as pure a fractional self-image as possible.

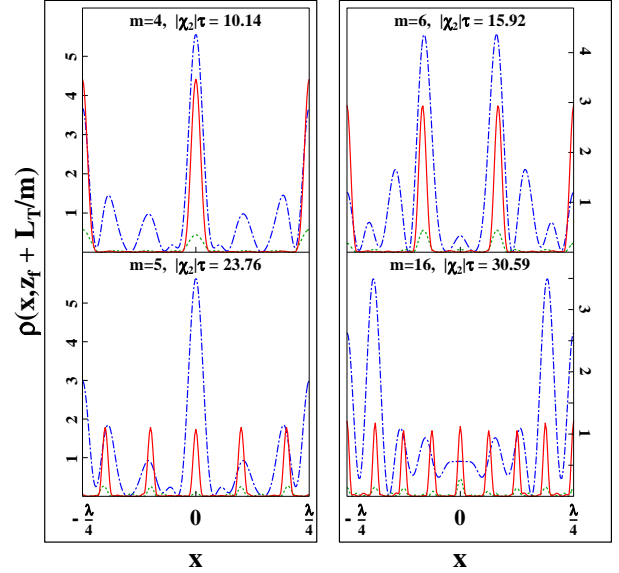


FIG. 3. The same type of density plots as those shown in Fig. 2, but for a moderate value of the upper state decay rate ($\gamma\tau = 4$) and a large value of the optical mask Rabi frequency $|\chi_2|/\gamma > 1$. The parameter $|\chi_2\tau|$ is chosen for each plot by requiring that the ratio of the maximum and minimum amplitudes of the peaks in the fractional density pattern are as close as possible to unity. In each case this choice produces the best n th-order fractional self-image with the filtered Talbot lens. For all plots, the focusing field area θ is equal to 10.

Chromatic aberration and atomic beam angular divergence degrade the focusing and the Talbot effect. Chromatic aberration arises as a result of a distribution of longitudinal velocities in the atomic beam. Recently, this effect was considered in detail for thin lens atom focusing [18]. It was shown that, owing to the finite depth of focus, the focusing is not seriously degraded for $\theta \approx 10$ until the spread in velocities divided by the average velocity, $\Delta v/u$, exceeds 0.1. For larger values of $\Delta v/u$, our numerical results indicate that high-order atomic gratings are still produced, but a background density arises whose amplitude starts to be comparable with the peaks of the fractional Talbot spots.

Angular divergence in the beam provides a more severe restriction. If atoms move at an angle ϕ relative to the z axis, the atomic distribution will be displaced by $\delta x \sim \phi L_T/m$ when the beam travels a distance equal to L_T/m . This displacement has to be smaller than the width of the peak in the focused atomic distribution if we want to maintain the beam flux and produce high-contrast, m th-order patterns. From Eq. (23b) one can deduce [18] that the half-width of the distribution is approximately equal to $0.06\lambda\theta^{-3/4}$. From this expression one finds that the angular divergence ϕ must be less than

$0.12 \frac{\lambda_{dB}}{\lambda} m\theta^{-3/4}$ for the FTL to operate effectively. This requirement is similar to the one necessary for the Talbot effect produced by microfabricated structures. We expect that the application of modern sub-recoil laser cooling techniques or the use of Bose condensates [23] will allow one to achieve these degrees of longitudinal and transverse cooling.

In summary, we have presented a proposal for creating nanostructures using both a focusing field and a masking field. The focusing field creates high density focal spots that are transmitted by the masking field. At the focal plane, the wave fronts entering the optical mask are coherent and fairly flat. Consequently, the situation is similar to a collimated beam that strikes the masking field. Owing to the Talbot effect, the spots are refocused with reduced periods following the masking field at distances that are integral fractions of the Talbot length. Using this technique, it should be possible to produce high contrast structures having periods as small as $\lambda/20$.

ACKNOWLEDGMENTS

J.L.C. is indebted to Prof. Tycho Sleator and the NYU Physics Department for providing him with the Visiting Scholar appointment during which this work was completed. This work is supported by the National Science Foundation under Grants No. PHY-9414020 and PHY-9800981 and by the U.S. Army Research Office under Grant No. DAAG55-97-0113 and AASERT No. DAAH04-96-0160.

-
- [1] M. Prentiss, G. Timp, N. Bigelow, R. E. Behringer, and J. E. Cunningham, *Appl. Phys. Lett.* **60**, 1027, (1992).
- [2] T. Sleator, T. Pfau, V. Balykin, and J. Mlynek, *Appl. Phys. B* **54**, 375, (1992).
- [3] R. E. Behringer, V. Natarajan, G. Timp, and D. M. Tennant, *J. Vac. Sci. Technol. B* **14**, 4072 (1996).
- [4] R. Gupta, J. J. McClelland, P. Marte, and R. J. Celotta, *Phys. Rev. Lett.* **76**, 4689 (1996).
- [5] K. K. Berggren, A. Bard, J. L. Wilbur, J. D. Gillapsy, A. G. Heig, J. J. McClelland, S. L. Rolston, W. D. Phillips, M. Prentiss, and G. W. Whitesides, *Science* **269**, 1255 (1995); R. Abfalterer, C. Keller, S. Bernet, M. K. Oberthaler, J. Schmiedmayer, and A. Zeilinger, *Phys. Rev. A* **56**, R4365 (1997); K. S. Johnson, J. H. Thywissen, N. H. Dekker, K. K. Berggren, A. P. Chu, R. Younkin, M. Prentiss, *Science* **280**, 1583 (1998).
- [6] B. Dubetsky, A. P. Kazantsev, V. P. Chebotayev, and V. P. Yakovlev, *Pis'ma Zh. Eksp. Teor. Fiz.* **39**, 531 (1984) [*JETP Lett.* **39**, 649 (1985)].
- [7] B. Dubetsky and P. R. Berman, *Phys. Rev. A* **50**, 4057 (1994).
- [8] S. B. Cahn, A. Kumarakrishnan, U. Shim, T. Sleator, P. R. Berman and B. Dubetsky, *Phys. Rev. Lett.* **79**, 784 (1997).
- [9] D. M. Giltner R. W. McGowan, and S. A. Lee, *Phys. Rev. Lett.* **75**, 2638 (1995).
- [10] P. R. Berman, B. Dubetsky, and J. L. Cohen, *Phys. Rev. A* **58**, 4801 (1998).
- [11] H. F. Talbot, *Philos. Mag.* **9**, 401 (1836).
- [12] M. S. Chapman, C. R. Ekstrom, T. D. Hammond, J. Schmiedmayer, B. E. Tannian, S. Wehinger, and D. E. Pritchard, *Phys. Rev. A* **51**, R14 (1995).
- [13] B. Dubetsky and P.R. Berman, in *Atom Interferometry*, edited by P.R. Berman, Academic Press, San Diego (1997), Chapter 10.
- [14] S. Nowak, Ch. Kurtsiefer, T. Pfau and C. David, *Opt. Lett.* **22**, 1430 (1997).
- [15] C. Keller, R. Abfalterer, S. Bernet, M. K. Oberthaler, J. Schmiedmayer, and A. Zeilinger, *J. Vac. Sci. Technol. B* **16**, 1998 (1998).
- [16] A. V. Turlapov, D. V. Strekalov, A. Kumarakrishnan, S. Cahn, and T. Sleator, *SPIE Proc.* **3736** (edited by A. V. Andreev, S. N. Bagayev, A. S. Chirkin, and V. I. Denisov), 26 (1999).
- [17] U. Janicke and M. Wilkens, *J. Phys. II (France)* **4**, 1975 (1994).
- [18] J. L. Cohen, B. Dubetsky and P. R. Berman, submitted to *Phys. Rev. A*, <http://xxx.lanl.gov/abs/physics/9907038>.
- [19] K. A. H. van Leeuwen, S. Meneghini, and W. P. Schleich, in the abstracts of the workshop "Atom optics applications," Les Houches, France, 1999, p. 19.
- [20] J. T. Winthrop and C. R. Worthington, *J. Opt. Soc. Am.*, **55**, 373 (1965).
- [21] A rectangular pulse is understood to have leading and falling edges with durations $\delta\tau$ large enough so that the adiabatic condition $\delta\tau \gg \min(\gamma^{-1}, |2\chi_2|^{-1}, |\Delta_2|^{-1})$ is satisfied.
- [22] Even for a large Rabi frequency $|\chi_2|$, one can still apply the Fourier method to derive an analog of Eq. (21) for the atom density at an arbitrary time $t - t_f$. To do this, instead of using an addition theorem for Bessel functions, one can use identity (121) of Ref. [13], valid for any periodic transmission function. This expression is not presented here.
- [23] M. Kozuma, L. Deng, E. W. Hagley, J. Wen, K. Helmerston, S. L. Rolston, and W. D. Phillips, *Phys. Rev. Lett.* **82**, 871 (1999); E. W. Hagley, L. Deng, M. Kozuma, J. Wen, K. Helmerston, S. L. Rolston, and W. D. Phillips, *Science* **283**, 1706 (1999).